JARO: 409–423 (2020)
DOI: 10.1007/s10162-020-00769-w

JARO
Journal of the Association for Research in Otolaryngology

Research Article

Utricular Sensitivity during Hydrodynamic Displacements of the Macula

Christopher John Pastras,[1] Sebastian Paolo Stefani,[1] Ian S Curthoys,[2] Aaron James Camp,[1] and Daniel John Brown[3]

[1]*The Meniere's Laboratory, School of Medical Sciences, The University of Sydney, Medical Foundation Building, 92-94 Parramatta Road, Camperdown, Sydney, New South Wales 2050, Australia*

[2]*Vestibular Research Laboratory, School of Psychology, The University of Sydney, Sydney, New South Wales 2050, Australia*

[3]*School of Pharmacy and Biomedical Sciences, Curtin University, Bentley, Western Australia 6102, Australia*

Received: 29 March 2020; Accepted: 31 July 2020; Online publication: 11 August 2020

ABSTRACT

To explore the effects of cochlear hair cell displacement, researchers have previously monitored functional and mechanical responses during low-frequency (LF) acoustic stimulation of the cochlea. The induced changes are believed to result from modulation of the conductance of mechano-electrical transduction (MET) channels on cochlear hair cells, along with receptor potential modulation. It is less clear how, or if, vestibular hair cell displacement affects vestibular function. Here, we have used LF (<20 Hz) hydrodynamic modulation of the utricular macula position, whilst recording functional and mechanical responses, to investigate the effects of utricular macula displacement. Measured responses included the Utricular Microphonic (UM), the vestibular short-latency evoked potential (VsEP), and laser Doppler vibrometry recordings of macular position. Over 1 cycle of the LF bias, the UM amplitude and waveform were cyclically modulated, with Boltzmann analysis suggesting a cyclic modulation of the vestibular MET gating. The VsEP amplitude was cyclically modulated throughout the LF bias, demonstrating a relative increase (~20–50 %; re baseline) and decrease (~10–20 %; re baseline), which is believed to be related to the MET conductance and vestibular hair cell sensitivity. The relationship between macular displacement and changes in UM and VsEP responses was consistent within and across animals. These results suggest that the sensory structures underlying the VsEP, often thought to be a cranial jerk-sensitive response, are at least partially sensitive to LF (and possibly static) pressures or motion. Furthermore, these results highlight the possibility that some of the vestibular dysfunction related to endolymphatic hydrops may be due to altered vestibular transduction following mechanical (or morphological) changes in the labyrinth.

Keywords: Utricle, Low-frequency biasing, Operating point, Endolymphatic hydrops, Meniere's

INTRODUCTION

Hearing sensitivity is modulated in the presence of a low-frequency (LF) acoustic tone (Deatherage and Henderson 1967; Zwicker 1977). This is believed to be caused by cyclic changes in the position of the basilar membrane (BM) and hair cells, stereocilia deflection, modulation of mechano-electrical transduction (MET) channel gating, movement of the MET Operating Point (OP) towards low-slope regions of the transduction curve, modulation of hair cell receptor potential, and ultimately modulation of the cochlear amplifier (Sachs and Hubbard 1981; Sellick et al. 1982; Patuzzi et al. 1984a; Rhode and Cooper 1993). Previous studies have examined the LF modulation of an array of cochlear responses, including intracellular

Correspondence to: Christopher John Pastras · The Meniere's Laboratory, School of Medical Sciences · The University of Sydney · Medical Foundation Building, 92-94 Parramatta Road, Camperdown, Sydney, New South Wales 2050, Australia. email: christopher.pastras@sydney.edu.au

and extracellular receptor potentials (Patuzzi and Sellick 1984; Russell and Kössl 1992; Cheatham and Dallos 1994), single-unit responses (Patuzzi et al. 1984b), compound action potentials (CAP) (Klis and Smoorenburg 1985), cochlear microphonics (CM) (Nieder and Nieder 1968a, 1968b; Pierson and Møller 1980), and otoacoustic emissions (Bian and Watts 2008; Brown et al. 2009; Brown and Gibson 2011; Lichtenhan 2012).

The functional loss associated with BM displacement has been suggested as the cause of the sensorineural hearing loss associated with pathologies such as endolymphatic hydrops (referred to here as 'hydrops'; (Tonndorf 1957), where hydrops is assumed to cause hydrostatic displacement of the BM towards the scala tympani (Brown and Gibson 2011). Experimentally inducing a *static* displacement of the BM can be difficult to induce reliably (Salt et al. 2009; Brown et al. 2013a), and thus, LF biasing has been used as a model of hydrodynamic displacement (Klis and Smoorenburg 1985; Sirjani et al. 2004; Brown et al. 2009; Salt and Plontke 2010). How, or if, hydrops affects peripheral vestibular function is less clear. The most common theory is that severe hydrops causes a rupture of the membranous labyrinth, and a subsequent ionic disturbance of the vestibular hair cells due to mixing of the endolymph and perilymph (Schuknecht 1976; Flock and Flock 2003; Kingma and Wit 2010). More recently, research has suggested hydrostatic displacement of vestibular hair cells, in the case of hydrops, may directly cause vestibular dysfunction (Rabbitt et al. 2001; Brown et al. 2013a; McGarvie et al. 2015). However, there is little evidence relating mechanical displacement of vestibular hair cells to functional changes. Here, we investigate the effect of LF biasing via hydrodynamic displacements of the utricular macula on utricular functional and mechanical responses, in vivo.

To monitor utricular function during LF biasing, we monitored the amplitude of the vestibular short-latency evoked potential (VsEP) evoked by bone-conducted vibration (BCV) pulses occurring at certain phases of the LF bias. The VsEP, recorded via the facial nerve canal, can be evoked either with the inner ear intact (using acoustic masking noise), or after surgical removal of the cochlea (Pastras et al. 2018b). Since the VsEP is a gross nerve response mediated by cranial jerk-sensitive hair cells (Jones et al. 2011; Pastras 2018), it was not clear if LF biasing of the macula would alter the VsEP (like the CAP is altered by LF tones) (Sellick et al. 1982).

In addition to the VsEP, we have monitored the Utricular Microphonic (UM) and utricular macular velocity using a laser Doppler vibrometer (Pastras 2018; Pastras et al. 2018a). These measures, which provide a more complete assessment of peripheral utricular function, require cochlear removal and direct access to the basal epithelium of the utricular macular. A previous study using a similar vestibular microphonic modulation, demonstrated a sigmoidal relationship between vestibular hair cell MET conductance and bundle displacement (Wit et al. 1988). To displace the utricular macula with a LF hydrodynamic bias, we then either directly applied hydrodynamic pressure to the vestibule via a fluid-filled pipette sealed into the horizontal semi-circular canal (when the cochlea was removed), or we stimulated the inner ear with LF air-conducted sound (ACS) via the ear canal (when the cochlea was intact). Importantly, with respect to LF ACS stimulation of the vestibular hair cells, the vestibular system is relatively insensitive to ACS (Young et al. 1977), because most of the hydro-acoustic energy is transmitted through the cochlea (Rosowski et al. 2004; Songer and Rosowski 2006). This can partly be overcome by surgically introducing a small third window into one of the semi-circular canals (SCCs), mimicking a semi-circular canal dehiscence (SCD) and causing pressure fluctuations to pass through the vestibule, thereby increasing its sensitivity to audio-frequency ACS (Vries and Bleeker 1949; Songer and Rosowski 2005).

The main aim of the present study was to use LF biasing of the utricular macula as a model of altered fluid pressure within the utricle to explore how, or if, changes in pressure alters utricular function and mechanics. Here, we show that LF biasing cyclically modulates utricular functional responses, but not macro-mechanical measures in the anaesthetized guinea pig.

METHODS

Animal Preparation and Surgery

Experiments were undertaken on 16 adult tri-coloured guinea pigs (*Cavia porcellus*) of either sex weighing between 300 and 500 g. All experimental protocols were approved by the University of Sydney Animal Ethics Committee. Animals initially received pre-anaesthetic intraperitoneal injections of atropine sulphate (Pfizer; 600 µg/ml) and temgesic (buprenorphine hydrochloride, Reckitt Benckiser, New Zealand; 324 µg/ml), and were thereafter anaesthetized in an induction chamber with isoflurane (2–4 %). Once sedated and lacking a foot-withdrawal reflex, guinea pigs were transported to the surgical table, mounted between custom-made ear bars, tracheotomized and artificially ventilated with a mixture of oxygen and isoflurane (2 %). Heart rate and SpO_2 levels were monitored, with the animal's core temperature regulated via a heating pad (Kent Scientific, CT, USA). Animals were electrically grounded via an electrode placed in the neck musculature.

For details regarding functional and mechanical recordings from the macular epithelium, see Pastras

et al. (2018a). In short, a ventral surgical approach was used to surgically ablate the cochlea and expose the utricular macula for localized micropipette recordings of the Utricular Microphonic and adjacent laser Doppler vibrometer (LDV) recordings of macular velocity. For details of VsEP recordings from the facial nerve canal, see Pastras et al. (2018b). Briefly, the dorsolateral bulla was opened, and an active Ag/AgCl electrode was inserted into the facial nerve canal in close proximity to the superior branch of the vestibular nerve. A reference electrode was inserted nearby in the neck musculature. Although the VsEP was the focus of these experiments, cochlear potentials (i.e. the CAP and CM) were recorded from the round window in selected animals. These were recorded in the process of chemically ablating cochlear function with potassium chloride (KCl; 250 mM) (discussed below) to demonstrate the vestibular origin of the VsEP. For the method used to record CAP thresholds, refer to Brown et al. (2018). In short, CAPs were evoked by 5 ms tone bursts (1 ms rise time) at 3, 6, 10, 14, and 18 kHz. Increasing stimulus levels (+5 dB) produced a linear regression fit of 6 samples. CAP thresholds were determined as the sound level where the CAP amplitude was zero. In select experiments, ~0.1 ml of 1.5 mM tetrodotoxin (TTX; Sigma Aldrich, Australia) was added to the vestibule to confirm the neurogenic origin of the VsEP.

Stimuli and Recordings

BCV stimuli were delivered to the skull via a Brüel & Kjær minishaker (Type 4810, Denmark) rigidly coupled to the contralateral earbar. A continuous, sinusoidal BCV stimulus was used to evoke the UM and a 0.6-ms duration BCV pulse was used to evoke the VsEP. A 3-axis accelerometer (bandpass 0.02–6 kHz; TE Connectivity, Ch-8200, Switzerland) was secured to the earbar to measure BCV acceleration.

Two methods were used to deliver a LF pressure to the utricle: (1) a direct hydrodynamic bias of the utricle after cochlear removal via a fluid tube coupled into the horizontal SCC (Fig. 1 and 2) an indirect hydrodynamic bias using LF ACS delivered by a speaker placed in the ear canal. For the direct hydrodynamic bias, a thin fluid-filled tube containing electrically inert and hydrophobic fluid (Fluorinert, FC-40, 3M St. Paul, MN, USA) was sealed into the horizontal SCC. An electrodynamic shaker (Yueqing Tenlee Electric Co., VT-500, China) was used to compress the fluid tube and modulate the hydrodynamic fluid pressure in the SCC. The magnitude of

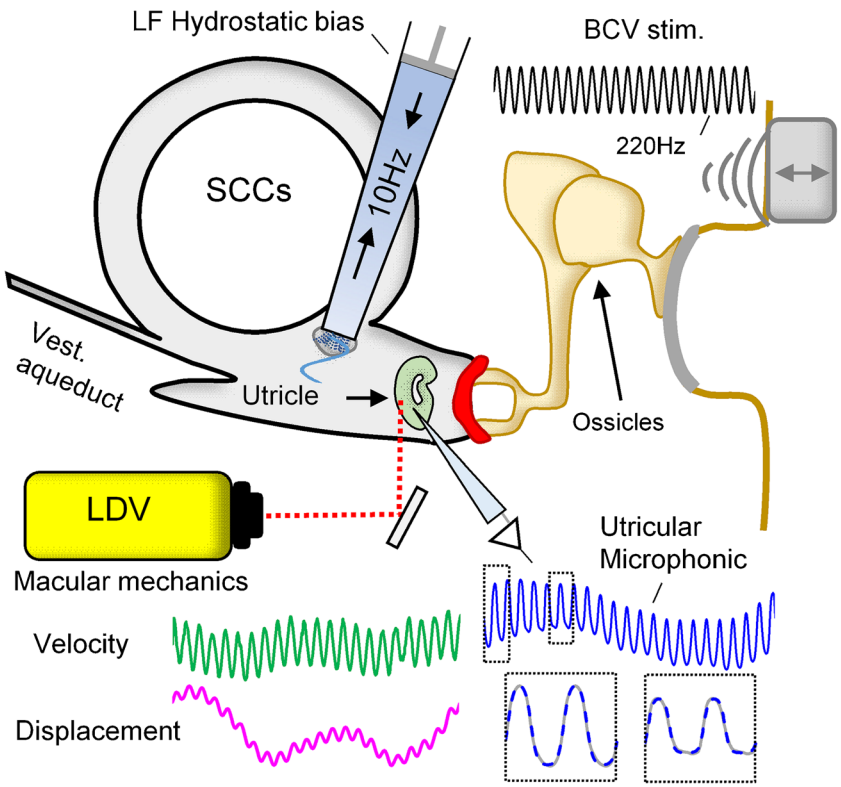

FIG. 1. Schematic of the method used to hydrodynamically displace the utricular macula. A fluid-filled pipette was sealed into the horizontal semi-circular canal, through which a 10-Hz AC pressure was applied. A continuous 220-Hz BCV stimulus was applied to the earbar, and the Utricular Microphonic was recorded from the basal surface of the macula using a glass microelectrode. Simultaneous recordings of macular velocity and displacement were performed using a laser Doppler vibrometer (LDV)

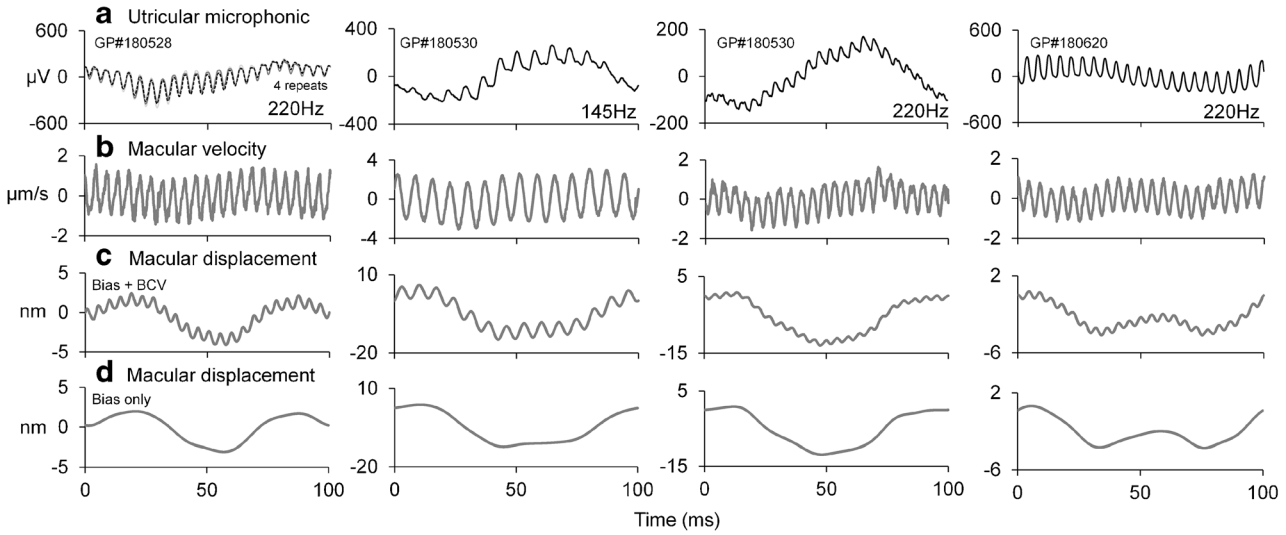

FIG. 2. **a** Simultaneous measurements of the UM (top row), **b** macular velocity (second row), and **c** and **d** macular displacement (with and without mid-frequency BCV components) during LF hydrodynamic biasing of the utricle in 3 animals. Each column is a recording from a different ear, or from a different animal (animal ID# shown in first row)

pressure applied was not measured. For the indirect ACS method, the cochlea and middle ear were kept intact. To chemically silence cochlear responses, ~0.1 ml of KCl (250 mM) was added to the round window, and a small hole (~0.1 mm Ø) was made in the apex, where a tissue wick was placed to draw KCl along the length of the cochlea. CAPs and VsEPs were monitored before, during, and after KCl perfusion to determine the efficacy of chemical ablation of cochlear function. Monitoring of VsEPs before and during cochlear ablation required broadband acoustic masking noise with a reasonably flat frequency response (±10 dB, 10 Hz to 18 kHz).

To enhance the vestibular systems sensitivity to LF ACS, a horizontal ($n = 5$) or anterior ($n = 3$) SCD was induced using a modified scalpel blade to shave the bony canal until slightly opened. With the cochlea intact but chemically silenced and the vestibular system more sensitive to ACS following SCD, a LF ACS (<20 Hz) was delivered to the ear canal via a silastic tube sealed into the ear canal and coupled to a modified 'sub-woofer' speaker acting as a volume velocity source. Again, the magnitude of the LF stimulus was not measured, as we were only interested in using the LF ACS to displace the utricular macula under non-physiological conditions.

All stimuli and responses were generated and recorded using customized LabVIEW programs (National Instruments, TX, USA). Stimuli were evoked using an external soundcard (SoundblasterX7, Creative Inc., Singapore). Physiological responses were amplified by 1000, with a 1-Hz to 10-kHz band-pass filter (IsoDAM, WPI, FL, USA) prior to being digitized at 40 kHz, 16-bit using an ADC (NI9205, National Instruments, TX, USA). For VsEP, UM, or macular vibration responses evoked once during a LF bias stimulus, recordings were averaged into 1 cycle of the LF stimulus. For VsEP responses evoked during the LF bias, the timing of the BCV pulse generating the VsEP, relative to the phase of the LF bias, was incrementally adjusted by 15 or 30°, starting at 0° and ending at 360°.

Boltzmann Analysis of the UM during the LF Bias

To examine changes in vestibular hair cell MET during the LF bias, we examined changes in the UM waveform (recorded via a glass microelectrode located close to the utricular hair cells, with minimal fluid in the vestibule) and assumed that the UM represents the current through the utricular MET channels and follows a Boltzmann activation function (Holton and Hudspeth 1986). A similar analysis has been used to analyse cochlear hair cell MET conductance using the CM (Patuzzi and Moleirinho 1998). At its simplest, the saturating UM waveform can be mathematically approximated using the following Boltzmann equation:

$$\mathrm{UM} = V_{\mathrm{off}} + \left(\frac{V_{\mathrm{sat}}}{\left(1 + \exp\left(Z \cdot \sin(2\pi f) + \mathrm{OP}\right)\right)} \right)$$

Here, V_{off} = a DC offset parameter, V_{sat} = the microphonic saturation voltage, Z = the sensitivity of the MET channels (slope of the transducer function), and OP = operating point (resting angle of the vestibular hair bundles prior to activation). The OP value was of primary interest, as it is dependent on several factors

such as macular compliance and changes in pressure. To convert the OP to a more intuitive value, reflecting MET channel conductance % (MET channels fully open or closed), we used the equation: MET $G\% = (V_{sat}/(1+\exp(OP)) * 100$. Boltzmann analysis was performed offline with a custom-made LabVIEW program using a Levenberg-Marquardt curve-fitting process to generate the Boltzmann parameters by a least-squares criterion. Every 2 cycles of the UM response were analysed, so when the UM was recorded during the presentation of a LF bias stimulus, changes in OP (MET G%) could be approximated during displacement of the utricular macula. Lissajous figures were produced by plotting the real UM against the assumed sinusoidal displacement of the stereocilia, including an estimate of the OP.

RESULTS

UM Modulation with Hydrodynamic Bias

A LF (5–20 Hz) hydrodynamic pressure delivered to the utricle resulted in a repeatable and cyclic modulation of the UM waveform (Fig. 2a). Simultaneous laser Doppler vibrometer (LDV) recordings revealed consistent LF modulation of macular velocity and displacement across different animals (Fig. 2b, c, and d). Specifically, the hydrodynamic bias resulted in a LF modulation of macular velocity by approximately 1–3 μm/s (Fig. 2b), whereas macular displacement was modulated by 5–20 nm, across animals (Fig. 2c and d). Importantly, for the stimulus that was evoking the UM there was no distortion of the macular velocity or displacement (Fig. 2b, c, and d).

To investigate if the UM waveform modulations were due to changes in the MET conductance of hair cells in the vicinity of the recording pipette, we compared the UM waveform when recorded from either side of the polarity reversal line of the utricular macula (Fig. 3a). A 220-Hz BCV stimulus (green), and 10-Hz hydrodynamic bias (blue; Fig. 3b) resulted in anti-phase UM potentials recorded from either side of the striola (lateral vs medial; *black* vs *red*), with opposite 'saturating effects' (Fig. 3b and c). For example, at ~270° of the LF bias, the lateral UM appeared to saturate at positive voltages, whereas the

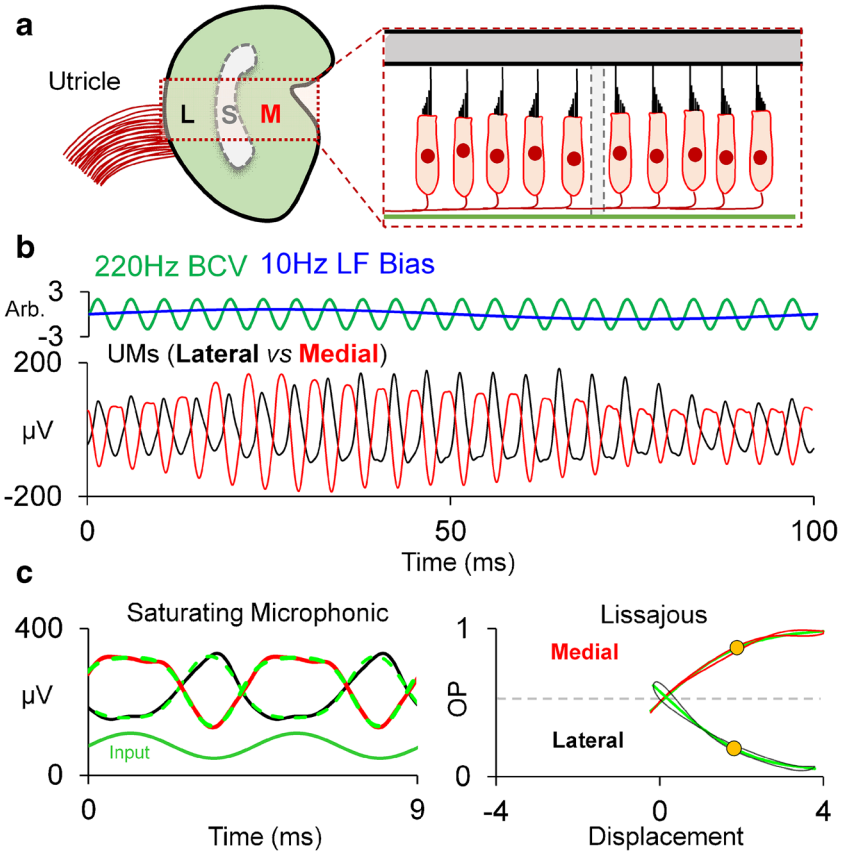

FIG. 3. **a** Schematic representation of the utricular macular, with lateral (L) and medial (M) recording positions from either side of the polarity reversal line. **b** A 220-Hz continuous BCV (green) and 10-Hz hydrodynamic bias (blue) stimulus resulted in a modulated UM waveform, recorded from either the lateral (black) or medial (red) areas of the macula. **c** The UM waveforms recorded from the lateral and medial locations, plotted relative to time (left) or relative to the BCV stimulus, with an additional assumed pseudo-static displacement of the macula (right)

medial UM saturated at negative voltages (Fig. 3b). This is further evident in the 2-cycle UM waveforms (Fig. 3c, *left*) and their corresponding Lissajous plots (Fig. 3c, *right*), which approximate the opening probability of the stereocilia responsible for generating the UM (Fig. 3c, *left*). For the 'medial UM' (*red*), the OP is biased in the 'opened' direction, whereas for the 'lateral UM' recording (black), the OP is biased 'closed'.

To quantify the changes in the UM response during the LF bias, every 2 cycles of the lateral and medial recorded UM waveforms were approximated using Boltzmann analysis (Fig. 4). The UM waveform was cyclically modulated over a single phase of the hydrodynamic bias, with clear changes in amplitude and saturation (Fig. 4a and d). UM responses were segmented into 2-cycle waveforms (Fig. 4b and e) and approximated with a Boltzmann function (dashed blue line). Lissajous plots of the UM versus the approximated displacement of the macula demonstrate cyclic modulations of the UM transducer OP shift over the LF bias (Fig. 4c and f). Importantly, Boltzmann analysis of UM recordings from either side of the polarity reversal line shows OP shifts that moved in the opposite direction of one another. That is, when the medial UM OP (Fig. 4c) increased, the lateral UM OP (Fig. 4f) decreased.

Measures of macular velocity and displacement associated with Fig. 4, obtained alongside the LF-biased UM recordings from either side of the polarity reversal line are shown in Fig. 5. Simultaneous recordings of the stimulus-frequency macular velocity (e.g. 200 Hz) during biasing demonstrated little modulation or distortion of the macular vibration during the hydrodynamic bias (Fig. 5a, c, d, and f). Importantly, recordings were performed on the same side of the polarity reversal line as that of the UM recordings. Displacement recordings suggest there was approximately a 5–10-nm LF displacement of the macula during the bias and that the phase of macular displacement was similar at both locations (Fig. 5b and e).

VsEP Evoked during Hydrodynamic Bias

In order to investigate the effect of LF utricular macular displacements on vestibular nerve sensitivity, the VsEP was measured during LF hydrodynamic biasing of the macula. Hydrodynamic biasing was achieved via a fluid-filled tube sealed into the horizontal SCC, with the cochlea intact (Fig. 6a–d), or after surgical cochlear removal (Fig. 6e–h). With the cochlea intact and using masking noise to suppress cochlear nerve responses to pulsed BCV

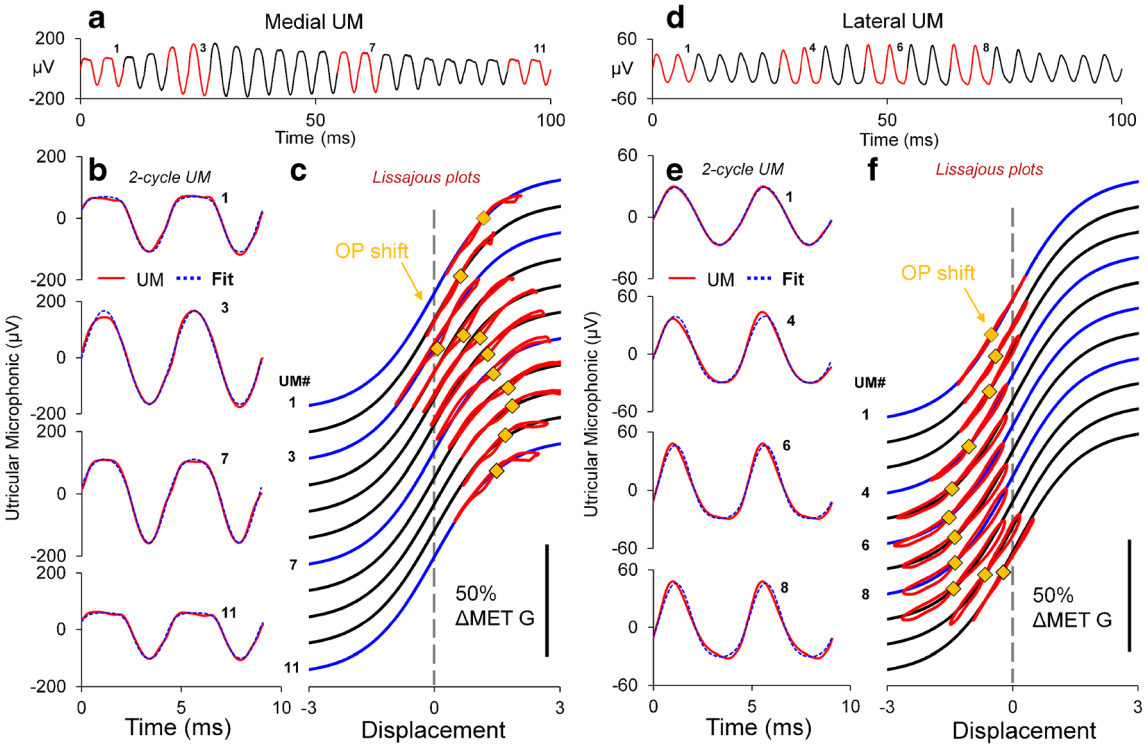

FIG. 4. **a** and **d** UM recordings from either side of the macula during a LF hydrodynamic bias. **b** and **e** UM waveforms (red) and Boltzmann approximation waveforms (blue). **c** and **f** UMs (red) plotted on a Boltzmann Lissajous curve representing MET channel gating, using the approximated macular displacement, which includes an estimate of the operating point (yellow squares; OP shift)

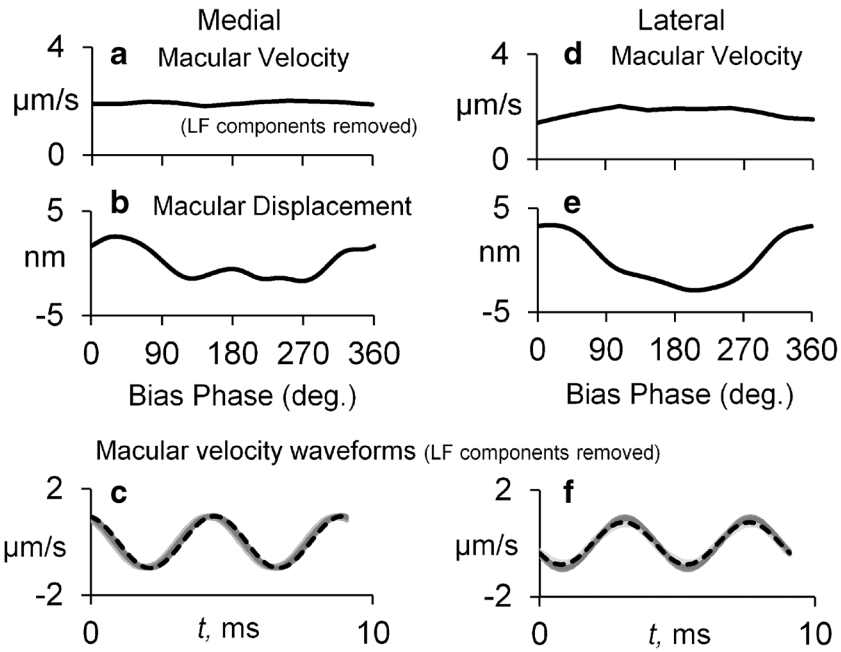

FIG. 5. Simultaneous macular macro-mechanical recordings associated with the medial and lateral UM measurements in Fig. 4a and d. **a** and **d** Simultaneous measurements of the 220-Hz macular velocity recorded using LDV from medial and lateral bead positions, respectively (LF bias components removed). **b** and **e** LF macular displacement during the bias. **c** and **f** Macular velocity waveforms associated with Fig. 5a and d

stimuli, the 20-Hz hydrodynamic bias resulted in a 20-Hz modulation of the potential recorded from the facial nerve canal (Fig. 6b). This likely reflected a cochlear microphonic, as it was not present following cochlear ablation (Fig. 6f). Removal of the 20-Hz components in the facial nerve canal recording permitted clearer visualization of the VsEP response at various phases of the LF bias (Fig. 6c and g). With

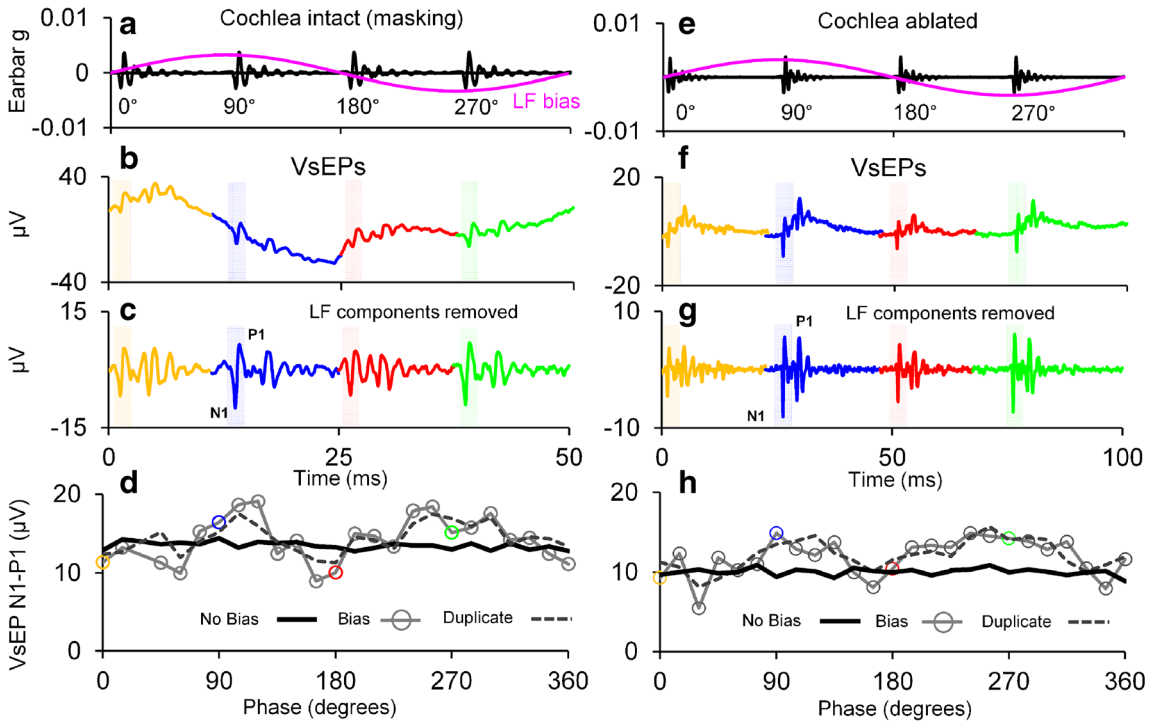

FIG. 6. **a** and **e** Earbar acceleration (black) during the LF hydrodynamic bias. **b** and **f** VsEPs recorded with the cochlear intact (left) or ablated (right), at 15-degree intervals of each cycle of the LF bias. VsEPs shown at 0° (yellow), 90° (blue), 180° (red) and 270° (green) of the LF hydrodynamic bias. **c** and **g** The same waveforms as **b** and **f**, with the LF components removed offline. **d** and **h** The VsEP N1-P1 amplitude during the LF bias, or without the bias

the cochlear intact, the VsEP N1-P1 amplitude was modulated by 90 % (~10 μV) during the bias (Fig. 6d, *grey and dashed lines*), whereas the VsEP amplitude was stable across multiple recordings without the LF bias (Fig. 6d, *black line*). With the cochlear ablated, LF biasing of the macula resulted in similar modulation of the VsEP, only without the additional LF components (Fig. 6f–h; note that here the LF bias was 10 Hz instead of 20 Hz). Interestingly, the VsEP amplitude mostly increased (~40 %) relative to baseline (Fig. 6d and h) throughout the bias. With the cochlea ablated, LDV measurements were used to quantify the level of macular velocity and displacement induced by the same 10 Hz hydrodynamic bias that caused VsEP modulation (Fig. 7). The average peak macular velocity modulation was 2 μm/s, whereas average peak macular displacement was 40 nm (Fig. 7). For comparison, displacements less than 10 nm were used to cause significant modulation of the UM waveform (Fig. 2).

To introduce LF modulation via air conduction, with the cochlear intact, a LF ACS was delivered to the inner ear via a speaker sealed into the ear canal, following chemical silencing of cochlear function and the surgical introduction of a SCD. A SCD was introduced to enhance ACS sensitivity of the vestibular system (Minor 2005; Dlugaiczyk et al. 2019). KCl was perfused because LF ACS produces relatively large cochlear potentials (Salt et al. 2013), which would otherwise dominate the recorded VsEP during LF biasing. To demonstrate that KCl perfusion of the scala tympani silenced cochlear but not vestibular receptors, CAP detection thresholds and VsEP responses were longitudinally monitored during KCl perfusion. CAP thresholds increased by more than 50 dB (Fig. 8a and b), and only the latter components of the VsEP were reduced, leaving the N1-P1 component of the VsEP largely unaltered (Fig. 8c). In all cases, supra-threshold CAP responses were irreversibly abolished >2 h after KCl exposure (Fig. 8a, *Inset*).

Following chemical silencing of the cochlea, acoustic masking noise did not change the amplitude or latency of the VsEP N1-P1 (data not shown). After KCl administration and the surgical introduction of a SCD, LF ACS delivered to the ear canal was used to acoustically bias the macula position which was found to be consistent within and across animals (Fig. 9 shows VsEP modulation in 4 animals). Depending on the level of the LF ACS, the average VsEP amplitude either increased and decreased once with the LF bias (Figs. 9 and 10a), or its amplitude increased and decreased twice during a single cycle of the LF bias in a 2-cycle pattern (Figs. 9 and 10c). Without the LF bias, the VsEP amplitude was not modulated (Figs. 9 and 10). As was observed with direct hydrodynamic biasing of the macula (Fig. 6), LF ACS

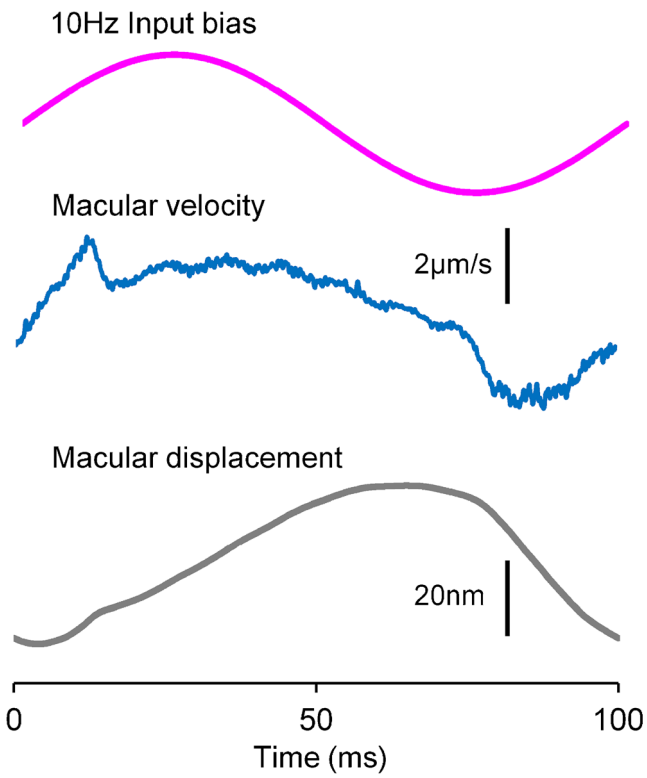

FIG. 7. Measurements of the macular velocity and displacement during a 10-Hz hydrodynamic bias (cochlear ablated; see Fig. 6 e–h)

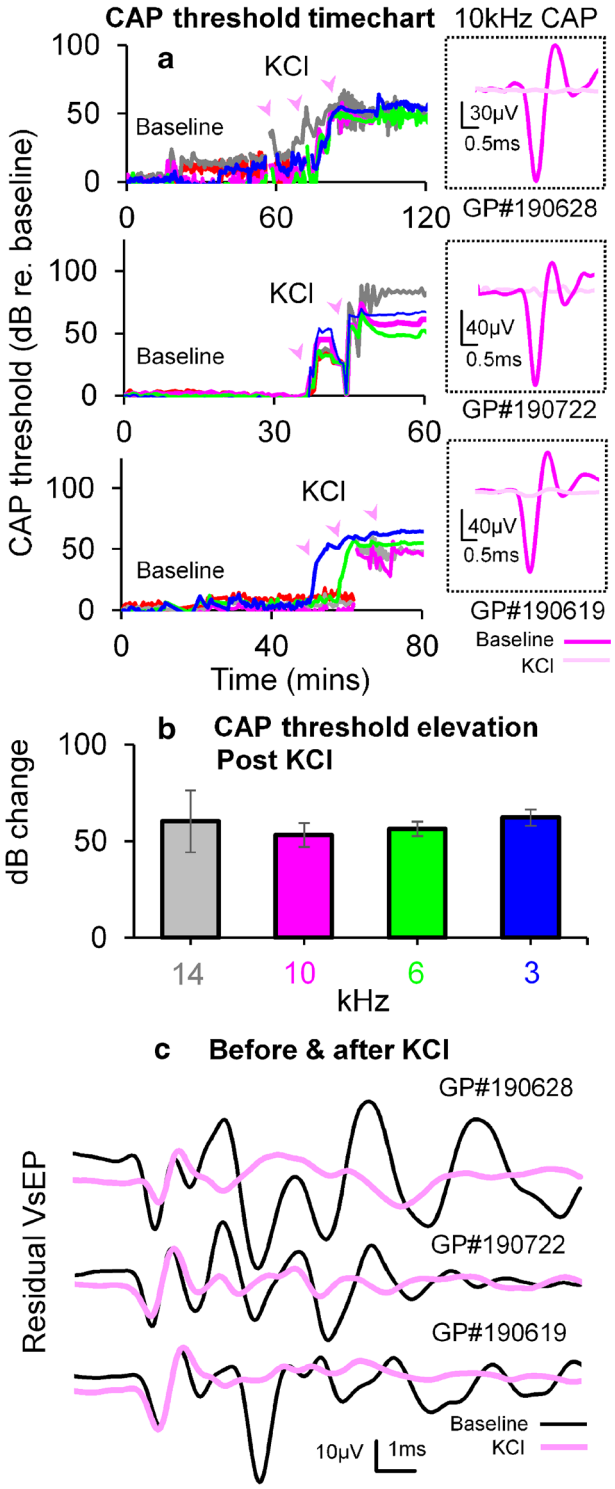

Fig. 8. **a** The change in CAP thresholds before and after KCl perfusion of the cochlea in 3 animals. *Inset*: CAP waveforms evoked by a 10-kHz tone burst before and >2 h after KCl. **b** Average CAP threshold increases after KCl across 3 animals. The 18-kHz change (red) is not shown as there was no response at any sound level after KCl. **c** The electrical response from the facial nerve canal to a BCV pulse, before and >2 h after KCl in 3 animals

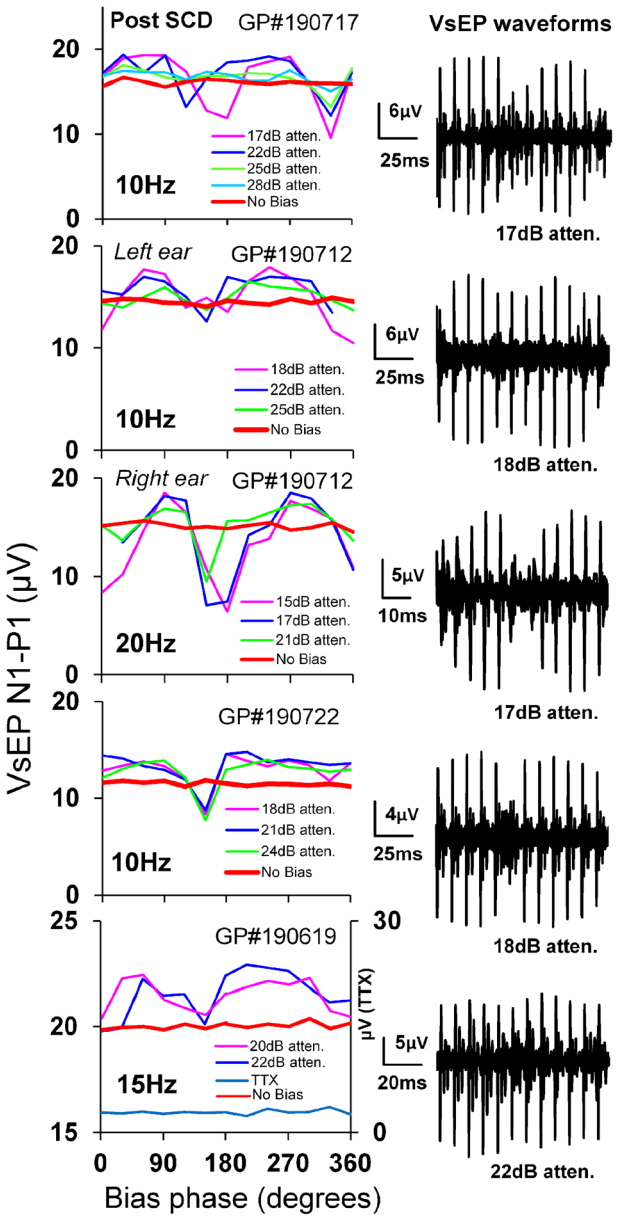

Fig. 9. *Left:* VsEP N1-P1 amplitude plotted over a cycle of the LF bias, in 4 animals using LF ACS following KCl ablation of the cochlea. Here, an SCD was used to enhance the sensitivity of the utricle to ACS. *Right*: VsEPs during LF ACS bias corresponding to the left panel. In GP#190619, TTX was applied to the round window, which abolished the VsEP

biasing also resulted in a net increase in the VsEP amplitude during the bias, relative to baseline (Fig. 10).

Here, we have interpreted the double modulation of the VsEP amplitude during the LF ACS bias as being caused by a modulation of the MET conductance through the 'zero' position on its transduction curve (the steepest part of the curve; Fig. 10b and d), with relatively small modulation of the MET conductance with the bias failing to drive the MET conduc-

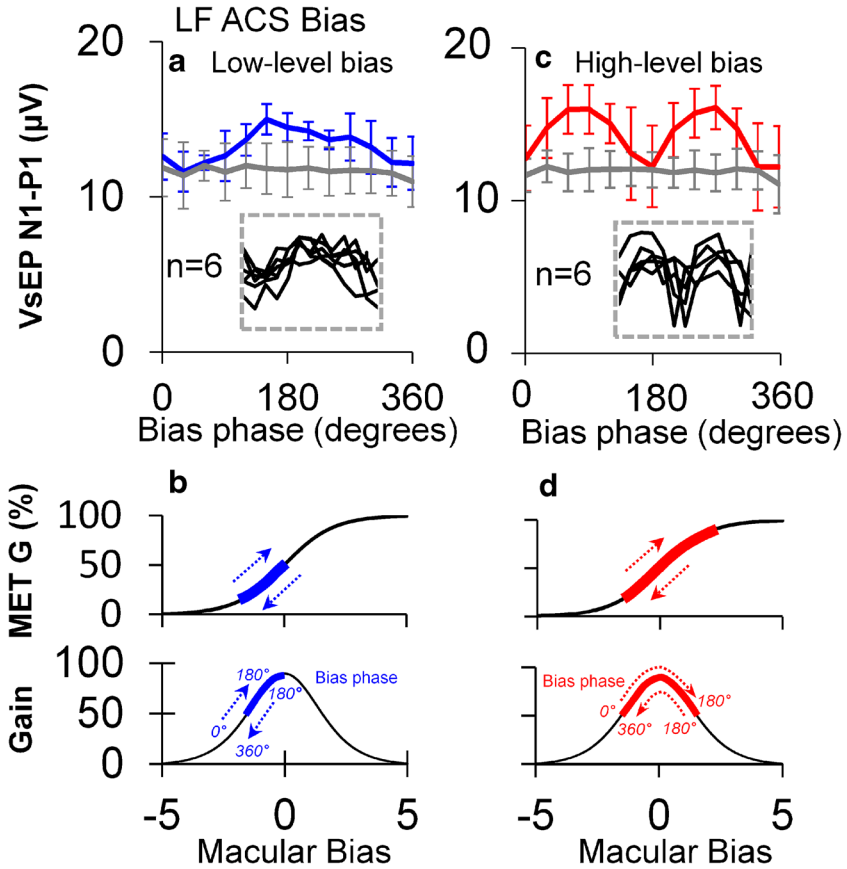

FIG. 10. **a** and **c** The VsEP amplitude during 1 cycle of a LF tone, presented at either a low (23–28 dB attenuation) or high (15–20 dB attenuation) sound level. Results have been averaged across 6 animals. *Inset*: Individual VsEP modulation in each animal. **b** and **d** A schematic of the assumed modulation of utricular hair cell MET conductance and gain during the LF bias, to explain the double modulation of the VsEP amplitude by high levels of a LF tone.

tance through this region of the transduction curve. That is, the amplitude of the VsEP and the sensitivity of the utricle to a BCV stimulus can be related to the slope of the transfer curve. A similar analysis of hearing sensitivity has been used to explain hearing threshold modulation during a LF tone (Kirk and Patuzzi 1997) and CAP amplitude modulation (Patuzzi 1987; Patuzzi 2011; Lichtenhan 2012).

DISCUSSION

The Effect of a Hydrodynamic Bias on Utricular Hair Cell Function and Mechanics

Results demonstrate reproducible utricular response modulation during each cycle of a hydrodynamic bias (Fig. 2). Importantly, macro-mechanical measurements of macular velocity suggest these bias-induced changes were not due to altered macular stiffness (Fig. 5a, c, d, and f). The UM amplitude and waveform were cyclically modulated during the bias, as was the VsEP amplitude, albeit in a more complex fashion. The UM changes were most likely due to changes in the MET OP, and 1 cycle of the bias caused one cyclic modulation of the OP (and MET G%). During 1 cycle of the LF bias, the VsEP amplitude typically displayed 2 cycles of amplitude modulation.

It should be noted that macular velocity was measured in the dorsoventral axis, which is perpendicular to the vector of maximum sensitivity for utricular hair bundle activation (Pastras et al. 2018a). Therefore, although the stiffness of the macular did not appear to be modulated during biasing, we cannot rule out non-linear macro-mechanical effects such as alterations in the magnitude of the neuroepithelial layer/otoconial layer shearing. However, we expect that such effects would predominantly result in changes in UM amplitude, rather than modulations in its waveform. The waveform changes, including effects on non-linear saturation, are more reflective of modulation in the MET channel gating (OP biasing) than sensitivity of the utricle to the BCV stimulus due to alterations in macular stiffness during the bias.

Further evidence that the bias-induced changes to the UM were due to OP modulation was provided by biased UM recordings from either side of polarity reversal line. As shown here and previously (Pastras et al. 2017), UM waveforms from either side of this line are anti-phase. This suggests that the BCV stimulus evoking the UM causes the macula to vibrate as a single, fixed structure with the morphological polarity of the hair cell stereocilia determining the phase of the MET conductance modulation during vibration. During a LF bias, it is also likely that the macula is displaced cyclically as a single structure, forcing MET channels on hair cells medial to the polarity reversal line to close when MET channels on hair cells lateral to the line are opening, and vice versa. The net result is an opposite effect of the bias on the asymmetric saturation of the UM waveform during the bias (Fig. 3). Note that all stimuli and response averages were locked in phase to a constant synch signal, ensuring that any response differences were physiological. The changes in the MET conductance of hair cells on either side of the polarity reversal line are more clearly illustrated in Fig. 4, where the UM was plotted against the assumed 220-Hz UM stimulus during the bias.

A potential source of error in the Boltzmann approximation of the UM waveform may relate to the contribution of vestibular nerve activity to the UM waveform. However, in several experiments, blocking nerve activity with TTX did not appreciably change the UM waveshape and had no effect on the approximated Boltzmann variables (data not shown; see Pastras et al. (2017); Pastras (2018)). In these experiments, nerve block irreversibly abolished the VsEP, which did not return after several hours, but did not alter the UM response.

The Effect of a Hydrodynamic Bias on Utricular Nerve Function

Previous studies have examined the effect of LF biasing on auditory nerve function (Sachs and Hubbard 1981; Sellick et al. 1982; Patuzzi et al. 1984b; Tono and Morizono 1995). Here we have used a LF hydrodynamic bias of the utricular macula, to examine utricular nerve function, or the VsEP. Two methods were used to hydrodynamically displace the utricular macula and modulate utricular nerve activity, though both produced similar results. First, with the cochlea surgically removed, a hydrodynamic pressure was directly applied to the SCC, similarly to that used for LF modulation of the UM, to induce a 40-nm cyclic modulation of the macula's position (Fig. 7). Second, with the cochlea intact, we utilized LF ACS to displace the macula because VsEP recordings do not require surgical cochlear removal to access the macula (as is the case for UM recordings). The purpose of this was to explore the effects of macular displacement with relatively less surgical modification of the inner ear. However, LF ACS biasing required the addition of a SCD to increase the utricle's sensitivity to ACS and chemical silencing of the cochlea to suppress cochlear responses. Moreover, with the cochlear intact, we were unable to measure macular velocity using laser Doppler vibrometry. Both modes of LF biasing of the utricular macula resulted in a complex 2-cycle modulation of the VsEP for each LF cycle (Figs. 6 and 9). Although the lowest levels of LF ACS that induced modulation produced a single-cycle modulation of the VsEP amplitude across 1 cycle of the bias (Fig. 10a).

Interestingly, LF modulation of the VsEP predominantly *increased* its amplitude during the bias (Fig. 10). The 2-cycle modulation of the VsEP amplitude and the average increase in the VsEP amplitude over the entirety of the bias may be explained by asymmetric MET channel gating. That is, theoretically, the hair cells should be most sensitive to a stimulus when the resting state of MET channels lie on the steepest part of the transfer curve (where the OP value is zero). If at rest, the MET channels are more closed than open (OP positioned low on the transfer curve), the hair cells are not operating at their most sensitive state. Biasing the MET channel gating towards the most sensitive state, and then beyond, would result in an increase and subsequent decrease in hair cell sensitivity. On return to their original state, there would again be an increase, and then decease in sensitivity. Such changes could explain the 2-cycle modulation of VsEP amplitude during a single cycle of a bias, as the MET channels are biased through their most sensitive state on the transfer curve (Fig. 10b and d). Moreover, if at rest, the MET channels do not exist at their most sensitive state (~50 % open), there should be an overall increase in the VsEP amplitude (Fig. 10). By comparison, modulations of the cochlear CAP with LF tones (Sellick et al. 1982; Patuzzi 2011; Lichtenhan 2012) display asymmetrical bias patterns, with greater CAP suppressions associated with displacements of the BM towards the scala tympani. It should be noted that there were intra-animal differences in the modulation of the VsEP amplitude, with some animals showing a predominant reduction of the VsEP during the LF bias (relative to baseline; Fig. 9, *Right ear*, GP#190712). It is plausible that such differences result from different resting conductances of the macular MET channels or that there were subtle differences in the resting MET channel conductance of hair cells in different regions of the macula and that our BCV stimulus evoking the VsEP differed across animals.

A Comparison of the Hydrodynamic Changes in Utricular Hair Cell and Neural Measures

Both the UM and VsEP were cyclically modulated during a LF hydrodynamic bias. However, there are fundamental differences in these response measures that should be discussed when considering how a LF hydrodynamic bias modulates utricular receptor function. For example, the UM is a relatively local measure of 'extrastriolar' hair cell activity, as 'striolar' hair cell activity largely cancels near the polarity reversal line, whilst the VsEP is a synchronized nerve response which arises from the 'jerk-sensitive' afferents at the striola (Pastras 2018). Thus, it is possible that differences in UM and VsEP modulation during a hydrodynamic bias may reflect specific differences in utricular hair cell transduction and mechanics (Nam et al. 2019). Indeed, morphological studies have demonstrated that mammalian type I hair cells at the striola are shorter and stiffer than type II extrastriolar hair cells, which appear tethered to the otoconial layer (Xue and Peterson 2006; Li et al. 2008; Spoon et al. 2011). Furthermore, recent recordings from our laboratory have demonstrated that UMs more closely follow macular displacement, whereas VsEPs are more sensitive to changes in macular (and cranial) jerk over other kinematic vectors (Pastras 2018). This suggests that the UM and VsEP may be evoked by different peripheral hair cell generators with different mechanical sensitivities.

Certainly in the cochlea, there are several distinct micromechanical activation modes, where the 'displacement-sensitive' outer hair cells are activated by the reticular lamina–tectorial membrane (RL-TM) shear and the viscously coupled inner hair cells are activated by longitudinal and radial fluid flow (Guinan Jr 2012) and also become entrained with partition displacement at higher frequencies due to viscous drag (Patuzzi and Yates 1987). Although, the micromechanical activation modes of vestibular hair bundles are not well defined, their differential architecture likely facilitates both displacement and viscous coupling, like the cochlea. It is important to note that the hydrodynamic bias (5–20 Hz) used in this study was much lower than the audio frequencies (>100 Hz) used to investigate the fluid activation of cochlear hair bundles. Ultimately, it is not clear if the vestibular hair bundles (particularly those which are free-standing and not embedded in the otoconial mass) are biased at 5 Hz by viscous drag, or by bulk or radial fluid flow, though it seems unlikely that if they are free-standing, they would be affected by static displacements of the macula. Importantly, that the level of macular velocity and displacement needed to modulate the VsEP was much larger than that of the UM suggests that the hair cells underlying the VsEP generation were likely velocity sensitive (i.e. their hair bundles were free-floating). Moreover, that the magnitude of macular velocity needed to modulate the VsEP was similar to the level of macular velocity needed to generate the UM (i.e. ~2 μm/s) suggests that the hair bundles generating the VsEP were being stimulated at the bias frequency (i.e. 5–20 Hz) in relation to the macular velocity, where the stereocilia were deflected due to viscous drag. Taken together, these results suggest that the 'VsEP hair bundles' are likely activated by macular (and hair cell) velocity, whereas the UM is activated by macular (and hair cell) displacement. If the striolar hair cells generating the VsEP are predominantly velocity-coupled and insensitive to hydrodynamic displacements of the macula, this poses an important question: How are these type I receptors effected by a LF bias? One mechanism could be direct voltage coupling in the utricle. For example, a LF hydrodynamic bias may only stimulate the displacement-sensitive extrastriolar utricular hair bundles, which may then cyclically modulate the small endovestibular potential above the viscously coupled utricular hair bundles (by several millivolts). This may then manipulate the basolateral resting membrane potential of nearby jerk-sensitive cells and result in cyclic modulations of afferent output (VsEP), as documented. Whilst this phenomenon has not been demonstrated in the vestibular system, in vivo, it has been well documented in the cochlea (Patuzzi and Sellick 1983a, 1983b; Patuzzi 2011). That is, there can be fairly dramatic changes in neural sensitivity with small alterations in endocochlear potential. Specific work investigating changes in vestibular nerve function whilst monitoring the endovestibular potential is required to test this hypothesis.

MET channel adaptation involving both fast and slow components (Wu et al. 1999; Vollrath and Eatock 2003) may also differentially affect the UM and VsEP due to changes in hair cell sensitivity, as demonstrated in the cochlea (Zhou and Nam 2019). Given the UM and bias stimuli are 'low-frequency' relative to the MET adaptation cut-off frequency, we can assume that the modulated UM response is operating on the 'adapted' state of MET gating, noting that the adaption is incomplete (Peng et al. 2013). How MET adaptation effects the VsEP is less clear, given it is evoked by a fast, transient jerk stimulus, where the MET channels are yet to fully (or even partially) adapt to the rapid hair bundle displacement.

LF Biasing as a Model for Hydrops

Although hydrostatic displacement of the organ of Corti affects cochlear sensitivity to sound and is a suggested cause of hearing loss associated with endolymphatic hydrops (Klis and Smoorenburg

1985; Brown et al. 2013b), it is not clear how hydrops affects balance function in Meniere's disease (MD). Several theories have been proposed to explain the cause of vertigo attacks surrounding hydrops such as a membrane rupture (Schuknecht 1976), altered hydrostatic pressure (Brown et al. 2013a), ischemia (Foster and Breeze 2013), and inflammation (Zhang et al. 2015). However, clinical observations and experimental findings mostly contradict these theories. For example, recent clinical work has demonstrated that a MD sufferer's vestibular reflex response to a dynamic stimulus (e.g. a rapid head turn or head tap) can be *increased* at the time of a vertigo attack (Manzari et al. 2010; Wen et al. 2012), whereas other responses such as a 'caloric response' can be reduced (McGarvie et al. 2015). Few, if any past theories explain why vestibular sensitivity may be enhanced during a vertigo attack and animal models mimicking membrane ruptures and ischemia have reported reductions in function (Elidan et al. 1986; Kingma and Wit 2010).

One experimental model to investigate the link between hydrops and inner ear dysfunction is the use of a static pressure bias, to mimic the hydropic ear (Bohmer 1993; Brown et al. 2013a). However, this experimental manipulation is hard to perform due to the difficulty in maintaining suitable pressure differences between the endolymph and perilymph due to the compliance of surrounding membranes and due to pressure shunting to nearby aqueducts (Salt and Plontke 2010). To avoid some of these issues, cochlear researchers have used LF biasing to produce quasi-static, cyclic displacements of the organ of Corti as a means to investigate changes in cochlear transduction as a model for hydrops (Klis and Smoorenburg 1985, 1988). Interestingly, results are similar to functional changes in the hydropic ear, with enhancements in the summating potential with displacements towards the scala tympani (Klis and Smoorenburg 1985; Tono and Morizono 1995) as well as modulations in the cochlear transducer operating point.

In this study, we have similarly biased the utricle using LF hydrodynamic pressure to investigate changes in utricular transduction and macromechanics as a model of utricular hydrops, where it is assumed that fluid pressure differences across the macula displaces the sensory structures of the utricle and alters its function.

Although utricular biasing has similarities to the LF biasing method used in the cochlea, there are several important differences to consider when interpreting results. In the cochlea, LF biasing is non-invasive and a relatively trivial technique, where a probe and bias tone are simultaneously delivered to the ear canal. Here, a loud, yet non-traumatic LF bias tone creates a differential pressure across the cochlear partition, which displaces the organ of Corti, and modulates the shearing of the outer hair cell stereocilia and indirectly modulates primary afferent activity through the cochlear amplifier. By comparison, LF biasing of the utricle is more complex. This requires more technical effort and invasive surgical procedures, which is likely to alter the resting hydrostatic pressure of the labyrinth. Unlike the cochlea, the activation of utricular hair bundles to BCV is more complicated and involves three-dimensional shearing between the otoconial mass and the neuro-epithelial layer. Changes in the fluid pressure within the vestibule can cause a gross displacement of the utricular macula, particularly if there is a slight pressure gradient across the macula (between the endolymph and perilymph), which may either create a simple axial displacement of the macula, or possibly a lateral motion of the macula epithelium, or some complex mixture of these modes. Both modes may result in a shearing of the hair bundle stereocilia, if the stereocilia motion does not, at these low frequencies, simply mirror hair bundle motion. Our present study suggests that, at the very least, axial displacement of the macula epithelium occurs, and it appears sufficient to explain the functional changes observed, such as modulation in the UM and VsEP, which are related to stereocilia shearing and MET channel gating modulation.

Of interest are the differences in macular motion needed to modulate the UM and the VsEP during LF biasing, which suggest differences in micromechanical activation modes between utricular hair cell subtypes across the macula. This has clinical relevance for understanding how various functional tests are differentially affected during hydrops, in particular, the commonly used vestibular evoked myogenic potential (VEMP). Given the VEMP is activated by type I hair cells and is the clinical analog of the VsEP, the result that the VsEP is sensitive to macular velocity suggests that the VEMP is likely insensitive to hydrostatic displacements of the macula, as may be expected to occur in the case of endolymphatic hydrops. Thus, the observed changes in the VEMP response observed during a Meniere's disease attack (Manzari et al. 2010) were probably not a reflection of macro-mechanical-induced changes in the sensitivity of the type I hair cells due to endolymphatic hydrops. The underlying cause of these changes remains obscure.

ACKNOWLEDGEMENTS

This work was supported by the Sydney Medical School Foundation at The University of Sydney, with funds raised by the Meniere's Research Fund Inc., and the Garnett Passe and Rodney Williams Memorial Foundation with support through a Junior Fellowship Grant. We thank Dr. Densil Cabrera and Mr. Jonothan Holmes from the University of

Sydney School of Architecture, Design and Planning for supplying the Ometron Laser Doppler Vibrometer.

REFERENCES

BIAN L, WATTS KL (2008) Effects of low-frequency biasing on spontaneous otoacoustic emissions: amplitude modulation. J Acoust Soc Am 123:887–898

BOHMER A (1993) Hydrostatic pressure in the inner ear fluid compartments and its effects on inner ear function. Acta Otolaryngol Suppl 507:3–24

BROWN DJ, GIBSON WP (2011) On the differential diagnosis of Meniere's disease using low-frequency acoustic biasing of the 2f1-f2 DPOAE. Hear Res 282:119–127

BROWN DJ, HARTSOCK JJ, GILL RM, FITZGERALD HE, SALT AN (2009) Estimating the operating point of the cochlear transducer using low-frequency biased distortion products. J Acoust Soc Am 125:2129–2145

BROWN D, CHIHARA Y, WANG Y (2013A) Changes in utricular function during artificial endolymph injections in guinea pigs. Hear Res 304:70–76

BROWN DJ, CHIHARA Y, CURTHOYS IS, WANG Y, BOS M (2013B) CHANGES IN COCHLEAR FUNCTION DURING ACUTE ENDOLYMPHATIC HYDROPS DEVELOPMENT IN GUINEA PIGS. HEAR RES 296:96–106

BROWN DJ, SOKOLIC L, FUNG A, PASTRAS CJ (2018) Response of the inner ear to lipopolysaccharide introduced directly into scala media. Hear Res 370:105–112

CHEATHAM MA, DALLOS P (1994) Stimulus biasing: a comparison between cochlear hair cell and organ of Corti response patterns. Hear Res 75:103–113

DEATHERAGE BH, HENDERSON D (1967) Auditory sensitization. The Journal of the Acoustical Society of America 42:438–440

DLUGAICZYK J, BURGESS AM, GOONETILLEKE SC, SOKOLIC L, CURTHOYS IS (2019) Superior canal dehiscence syndrome: relating clinical findings with vestibular neural responses from a guinea pig model. Otology & neurotology : official publication of the American Otological Society, American Neurotology Society [and] European Academy of Otology and Neurotology 40:e406–e414

ELIDAN J, LIN J, HONRUBIA V (1986) The effect of loop diuretics on the vestibular system. Assessment by recording the vestibular evoked response Archives of otolaryngology–head & neck surgery 112:836–839

FLOCK Å, FLOCK B (2003) Micro-lesions in Reissner's membrane evoked by acute hydrops. Audiology and Neurotology 8:59–69

FOSTER CA, BREEZE RE (2013) The Meniere attack: an ischemia/reperfusion disorder of inner ear sensory tissues. Med Hypotheses 81:1108–1115

GUINAN JJ JR (2012) How are inner hair cells stimulated? Evidence for multiple mechanical drives. Hear Res 292:35–50

HOLTON T, HUDSPETH AJ (1986) The transduction channel of hair cells from the bull-frog characterized by noise analysis. J Physiol 375:195–227

JONES TA, JONES SM, VIJAYAKUMAR S, BRUGEAUD A, BOTHWELL M, CHABBERT C (2011) The adequate stimulus for mammalian linear vestibular evoked potentials (VsEPs). Hear Res 280:133–140

KINGMA CM, WIT HP (2010) The effect of changes in perilymphatic K+ on the vestibular evoked potential in the guinea pig. European archives of oto-rhino-laryngology : official journal of the European Federation of Oto-Rhino-Laryngological Societies (EUFOS) : affiliated with the German Society for Oto-Rhino-Laryngology - Head and Neck Surgery 267:1679–1684

KIRK DL, PATUZZI RB (1997) Transient changes in cochlear potentials and DPOAEs after low-frequency tones: the 'two-minute bounce' revisited. Hear Res 112:49–68

KLIS JF, SMOORENBURG GF (1985) Modulation at the guinea pig round window of summating potentials and compound action potentials by low-frequency sound. Hear Res 20:15–23

KLIS JF, SMOORENBURG GF (1988) Cochlear potentials and their modulation by low-frequency sound in early endolymphatic hydrops. Hear Res 32:175–184

LI A, XUE J, PETERSON EH (2008) Architecture of the mouse utricle: macular organization and hair bundle heights. J Neurophysiol 99:718–733

LICHTENHAN JT (2012) Effects of low-frequency biasing on otoacoustic and neural measures suggest that stimulus-frequency otoacoustic emissions originate near the peak region of the traveling wave. J Assoc Res Otolaryngol 13:17–28

MANZARI L, TEDESCO AR, BURGESS AM, CURTHOYS IS (2010) Ocular and cervical vestibular-evoked myogenic potentials to bone conducted vibration in Meniere's disease during quiescence vs during acute attacks. Clinical neurophysiology : official journal of the International Federation of Clinical Neurophysiology 121:1092–1101

MCGARVIE LA, CURTHOYS IS, MACDOUGALL HG, HALMAGYI GM (2015) What does the dissociation between the results of video head impulse versus caloric testing reveal about the vestibular dysfunction in Ménière's disease? Acta Otolaryngol 135:859–865

MINOR LB (2005) Clinical manifestations of superior semicircular canal dehiscence. Laryngoscope 115:1717–1727

NAM JH, GRANT JW, ROWE MH, PETERSON EH (2019) Multiscale modeling of mechanotransduction in the utricle. J Neurophysiol 122:132–150

NIEDER P, NIEDER I (1968A) Some effects of tonal interactions as seen in the cochlear microphonic. The Journal of the Acoustical Society of America 43:1092–1106

NIEDER P, NIEDER I (1968B) Studies of two-tone interaction as seen in the guinea pig microphonic. The Journal of the Acoustical Society of America 44:1409–1422

PASTRAS CJ (2018) Assessment of utricular nerve, Hair Cell and Mechanical function, in vivo

PASTRAS C, CURTHOYS I, BROWN D (2017) In vivo recording of the vestibular microphonic in mammals. Hear Res 354:38–47

PASTRAS CJ, CURTHOYS IS, BROWN DJ (2018A) Dynamic response to sound and vibration of the guinea pig utricular macula, measured in vivo using laser Doppler Vibrometry. Hear Res 370:232–237

PASTRAS CJ, CURTHOYS IS, SOKOLIC L, BROWN DJ (2018B) Suppression of the vestibular short-latency evoked potential by electrical stimulation of the central vestibular system. Hear Res 361:23–35

PATUZZI RB (1987) A model of the generation of the cochlear microphonic with nonlinear hair cell transduction and nonlinear basilar membrane mechanics. Hear Res 30:73–82

PATUZZI R (2011) Ion flow in cochlear hair cells and the regulation of hearing sensitivity. Hear Res 280:3–20

PATUZZI R, MOLEIRINHO A (1998) Automatic monitoring of mechano-electrical transduction in the guinea pig cochlea. Hear Res 125:1–16

PATUZZI R, SELLICK PM (1983A) The alteration of the low frequency response of primary auditory afferents by cochlear trauma. Hear Res 11:125–132

PATUZZI R, SELLICK PM (1983B) A comparison between basilar membrane and inner hair cell receptor potential input-output functions in the guinea pig cochlea. J Acoust Soc Am 74:1734–1741

PATUZZI R, SELLICK P (1984) The modulation of the sensitivity of the mammalian cochlea by low frequency tones II. Inner hair cell receptor potentials. Hearing research 13:9–18

Patuzzi RB, Yates GK (1987) The low-frequency response of inner hair cells in the guinea pig cochlea: implications for fluid coupling and resonance of the stereocilia. Hear Res 30:83–98

Patuzzi R, Sellick P, Johnstone B (1984a) The modulation of the sensitivity of the mammalian cochlea by low frequency tones. III. Basilar membrane motion. Hearing research 13:19–27

Patuzzi R, Sellick PM, Johnstone BM (1984b) The modulation of the sensitivity of the mammalian cochlea by low frequency tones. I. Primary afferent activity. Hear Res 13:1–8

Peng AW, Effertz T, Ricci AJ (2013) Adaptation of mammalian auditory hair cell mechanotransduction is independent of calcium entry. Neuron 80:960–972

Pierson M, Møller A (1980) Effect of modulation of basilar membrane position on the cochlear microphonic. Hear Res 2:151–162

Rabbitt R, Yamauchi A, Boyle R, Highstein S (2001) How endolymph pressure modulates semicircular canal primary afferent discharge. Ann N Y Acad Sci 942:313–321

Rhode WS, Cooper NP (1993) Two-tone suppression and distortion production on the basilar membrane in the hook region of cat and guinea pig cochleae. Hear Res 66:31–45

Rosowski JJ, Songer JE, Nakajima HH, Brinsko KM, Merchant SN (2004) Clinical, experimental, and theoretical investigations of the effect of superior semicircular canal dehiscence on hearing mechanisms. Otology & Neurotology 25:323–332

Russell IJ, Kössl M (1992) Modulation of hair cell voltage responses to tones by low-frequency biasing of the basilar membrane in the guinea pig cochlea. J Neurosci 12:1587–1601

Sachs MB, Hubbard AE (1981) Responses of auditory-nerve fibers to characteristic-frequency tones and low-frequency suppressors. Hear Res 4:309–324

Salt AN, Plontke SK (2010) Endolymphatic hydrops: pathophysiology and experimental models. Otolaryngol Clin N Am 43:971–983

Salt AN, Brown DJ, Hartsock JJ, Plontke SK (2009) Displacements of the organ of Corti by gel injections into the cochlear apex. Hear Res 250:63–75

Salt AN, Lichtenhan JT, Gill RM, Hartsock JJ (2013) Large endolymphatic potentials from low-frequency and infrasonic tones in the guinea pig. J Acoust Soc Am 133:1561–1571

Schuknecht H (1976) Pathophysiology of endolymphatic hydrops. Archives of oto-rhino-laryngology 212:253–262

Sellick P, Patuzzi R, Johnstone B (1982) Modulation of responses of spiral ganglion cells in the guinea pig cochlea by low frequency sound. Hear Res 7:199–221

Sirjani DB, Salt AN, Gill RM, Hale SA (2004) The influence of transducer operating point on distortion generation in the cochlea. J Acoust Soc Am 115:1219–1229

Songer JE, Rosowski JJ (2005) The effect of superior canal dehiscence on cochlear potential in response to air-conducted stimuli in chinchilla. Hear Res 210:53–62

Songer JE, Rosowski JJ (2006) The effect of superior-canal opening on middle-ear input admittance and air-conducted stapes velocity in chinchilla. The Journal of the Acoustical Society of America 120:258–269

Spoon C, Moravec WJ, Rowe MH, Grant JW, Peterson EH (2011) Steady-state stiffness of utricular hair cells depends on macular location and hair bundle structure. J Neurophysiol 106:2950–2963

Tonndorf J (1957) The mechanism of hearing loss in early cases of endolymphatic hydrops. The Annals of otology, rhinology, and laryngology 66:766–784

Tono T, Morizono T (1995) Low-frequency biasing of round window responses in guinea pigs and chinchillas. Audiology : official organ of the International Society of Audiology 34:47–56

Vollrath MA, Eatock RA (2003) Time course and extent of mechanotransducer adaptation in mouse utricular hair cells: comparison with frog saccular hair cells. J Neurophysiol 90:2676–2689

Vries HD, Bleeker JD (1949) The microphonic activity of the labyrinth of the pigeon: part II: the response of the cristae in the semicircular canals. Acta Otolaryngol 37:298–306

Wen MH, Cheng PW, Young YH (2012) Augmentation of ocular vestibular-evoked myogenic potentials via bone-conducted vibration stimuli in Meniere disease. Otolaryngology–head and neck surgery : official journal of American Academy of Otolaryngology-Head and Neck Surgery 146:797–803

Wit H, Tideman B, Segenhout J (1988) Modulation of microphonics: a new method to study the vestibular system. In: clinical testing of the vestibular system. Karger publishers, pp 59–64

Wu YC, Ricci AJ, Fettiplace R (1999) Two components of transducer adaptation in auditory hair cells. J Neurophysiol 82:2171–2181

Xue J, Peterson EH (2006) Hair bundle heights in the utricle: differences between macular locations and hair cell types. J Neurophysiol 95:171–186

Young ED, Fernández C, Goldberg JM (1977) Responses of squirrel monkey vestibular neurons to audio-frequency sound and head vibration. Acta Otolaryngol 84:352–360

Zhang J, Chen S, Hou Z, Cai J, Dong M, Shi X (2015) Lipopolysaccharide-induced middle ear inflammation disrupts the cochlear intra-strial fluid-blood barrier through down-regulation of tight junction proteins. PLoS One 10:e0122572

Zhou W, Nam J-H (2019) Probing hair cell's mechano-transduction using two-tone suppression measurements. Sci Rep 9:4626

Zwicker E (1977) Masking-period patterns produced by very-low-frequency maskers and their possible relation to basilar-membrane displacement. The Journal of the Acoustical Society of America 61:1031–1040